Available online at www.sciencedirect.com

ScienceDirect

Energy Procedia 137 (2017) 307–314

Energy Procedia

www.elsevier.com/locate/procedia

14th Deep Sea Offshore Wind R&D Conference, EERA DeepWind'2017, 18-20 January 2017, Trondheim, Norway

Experimental study on power curtailment of three in-line turbines

Jan Bartl[a]*, Yaşar Ostovan[b], Oguz Uzol[b], Lars Sætran[a]

[a] *Department of Energy and Process Eng., Norwegian University of Science and Technology, Kolbjørn Hejes vei 2, 7491 Trondheim, Norway*
[b] *METU Center for Wind Energy, Department of Aerospace Engineering, Middle East Technical University, 06800 Çankaya Ankara, Turkey*

Abstract

A dataset of wind tunnel power and wake flow measurements on a setup of three aligned model wind turbines is presented. The power outputs of the three turbines are in good agreement with measurements from a full-scale wind farm of similar inter-turbine spacing. A comparison of the wake flow behind the first row and the second row shows a significantly higher mean velocity loss behind the second row justifying a further power drop from the second to the third row turbine. Curtailing the front row turbine to smaller than rated tip speed ratios resulted in insignificant total power gains below 1%. Curtailments of both the first and second row turbine indicate that the best combined array power results are achieved for slightly lower than rated tip speed ratios. Although power curtailment is observed to have a rather small potential for power optimization of a wind farm, it could be an effective method for load distribution at constant farm power.

Peer-review under responsibility of SINTEF Energi AS.

Keywords: Wind turbine wake; Wind farm control; Induction-based wake control, Power curtailment.

1. Introduction

Depending on the inter-turbine spacing, wake interactions between individual turbines are estimated to cause power losses up to 10-20% in large offshore wind farms [1]. Therefore, holistic wind farm control approaches are proposed to optimize the farm's capability of kinetic energy extraction from the wind [2]. Wind farm control methods can, in general, be classified as wake deflection methods like yaw control or axial induction based control

* Corresponding author. Tel.: +47 73593714
E-mail address: jan.bartl@ntnu.no

1876-6102
Peer-review under responsibility of SINTEF Energi AS.
10.1016/j.egypro.2017.10.355

methods like pitch or torque control of the upstream turbines. Even though the potential for power gains by wake deflection control is estimated to be larger [3], [4], axial induction based curtailment methods have the advantage of a more uniform load distribution over the downstream turbine rotor area. Depending on the turbine type, inter-turbine spacing, and the site-specific wind conditions, axial-induction based control is therefore considered an effective option for power and load control in tightly spaced wind farms.

By reducing the induction of the upstream turbine through tip speed ratio or pitch control, more kinetic energy is left in the wake flow that can be used by the downstream turbines. A previous study by Bartl and Sætran [5] of induction based control on two in-line turbines indicates a higher potential for power gains for tip speed ratio control than for pitch control. An investigation by Hansen et al. [6] highlights that the level of atmospheric turbulence intensity significantly influences the wake recovery and thus the total power output of a wind farm. This is confirmed in a model scale study by Ceccotti et al. [7], in which a curtailment of the first row is shown to be effective for low background turbulence and small turbine separation distances ($\leq$ 3D) only. However, the potential power increase for a two turbine arrangement is observed to be within one percent. In full-scale wind farms measurements on aligned turbines show the biggest power drop between the first and second row [1], [6], [8]. The difference in power production from the second to the third row is considerably smaller, which leads to a more or less stable production for turbine rows located even further downstream. The additional energy extraction by rotors from the third row on seems to be balanced by the entrainment of high kinetic energy fluid from the surrounding freestream flow. Therefore, an investigation of two aligned turbines may not be conclusive for an entire wind farm as also the third turbine power output and further rows could be affected by a curtailment of the front row turbine. In a Large-Eddy-Simulation (LES) of the tightly spaced Lillgrund wind farm Nilsson et al. [9] investigate the potential for increasing the wind farm production by curtailment of the front row turbines. By pitching out the front row turbines, they could not observe a positive contribution to the overall wind farm power production. Another CFD study based on the actuator line technique by Mikkelsen et al. [10] on a row of three aligned turbines shows increased production of the second and third turbine for a pitched first row turbine.

In this collaborative experiment between the Norwegian University of Science and Technology (NTNU) and Middle East Technical University (METU) Center for Wind Energy, measurements on three aligned model wind turbines of identical rotor geometry are carried out. It is investigated whether a curtailment of the first and second row can benefit the combined power output of a row of three aligned wind turbines.

2. Methodology

2.1. Wind tunnel, model turbines and rotor geometry

The test section of the closed-loop wind tunnel at NTNU in Trondheim is 2.71m wide, 1.81m high and 11.15m long. Static pressure holes are installed at two defined circumferences at the inlet of the tunnel in order to control the inflow speed. The wind tunnel is driven by a 220kW fan, which is located behind the test section. The model wind farm consists of the first row turbine (T1) from NTNU and the second (T2) and third row turbine (T3) from METU. The turbines have the exactly same rotor and nacelle geometry. The three-bladed rotors have a diameter of D=0.944 m and turn in the counter-clockwise direction. The rotors are controlled by systems of electric motors and frequency inverters by Siemens (T1, NTNU) respectively Panasonic (T2 & T3, METU). The turbines' rotational speed can be controlled up to about 3500 rpm, while the extensive power is consumed by external load resistances. The turbine blades are based on the NREL S826 airfoil and precision milled in aluminum. Three different sets of experimental performance data of the NREL S826 airfoil for low Reynolds numbers can be found in publications by Ostovan et al. [11], Sarmast and Mikkelsen [12] and Sagmo et al. [13], all of which can be used as input data for Blade Element Momentum (BEM) simulations.

2.2. Experimental setup

Fig.1 shows a side-view of the wind tunnel with the three model turbines installed. The first row turbine (T1) is mounted 2.00D from the tunnel inlet, while turbines T2 and T3 are set up with an inter-turbine spacing of 3.00D.

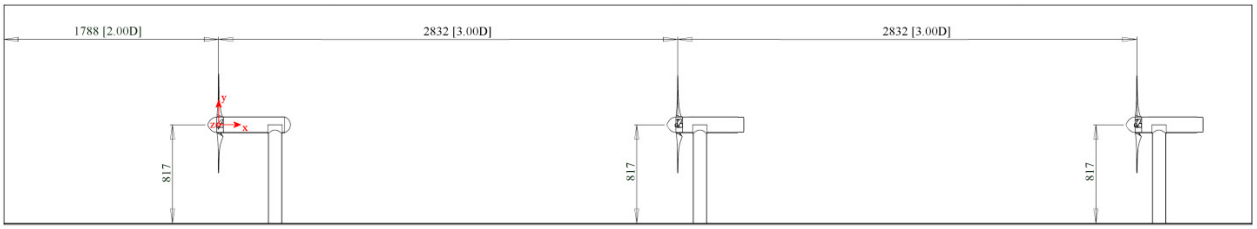

Fig. 1. Setup of the turbines in the wind tunnel and reference coordinate system

The turbine hub height is h_{hub}=817mm, which is slightly below the wind tunnel center. The figure also shows the reference coordinate system with its origin in the center of the first turbine rotor plane. The turbines are exposed to a uniform inflow of u_{ref}=11.5m/s. The turbulence intensity in the inflow is measured to be TI=0.23% at the first row turbine location. The design tip speed ratio of all three turbines is λ=6.0 which is giving an optimal axial induction factor of $a \approx 0.33$ at r/R=0.8.

In order to study the effect of variations in tip speed ratio of the first and second row turbines on the total array power, the first row turbine is set to discrete tip speed ratios λ_{T1}=[4.5, 5.0, 5.5, 6.0, 6.5]. Meanwhile, 15 tip speed ratios each in steps of $\Delta\lambda_{T2}=\Delta\lambda_{T3}$=0.20 around the optimum operation point are automatically scanned for the second and third turbine.

2.3. Measurement instrumentation and settings

All three turbines are equipped with in-nacelle torque transducers and optical cells for an acquisition of the rotational speed. Torque and rotational speed are averaged over 30s and the mechanical power on the rotor shaft calculated. The statistical uncertainty of the power coefficient of T1 at λ=6.0 is calculated to be lower than ±3.0%.

Wake flow measurements are carried out x/D=3 behind the first row turbine T1 without T2 and T3 being installed and x/D=3 behind T2, without T3 being installed. These locations are exactly the same locations of T2 respectively T3 and therefore represent the wake flow these turbines are exposed to. The velocity measurements are performed using a Laser Doppler Anemometer (LDA) by Dantec Dynamics. The statistical uncertainties of the mean velocities are calculated to be lower than ±0.5% considering a 95% confidence interval.

3. Results

3.1. Power output of the turbine array

In a first test all three aligned turbines are individually controlled to their optimum power point. The three turbines have identical C_P-λ characteristics with a maximum power coefficient $C_{P,max}$=0.462 at rated tip speed ratio λ_{opt}=6.0 when exposed to the undisturbed freestream flow. When operated in the wake of one or more upstream turbines the power coefficients of the second and third row turbines are reduced to $C_{P,T2}$=0.121 and $C_{P,T2}$=0.088, respectively, as shown in Fig.2 (a). The C_P-λ characteristics are all referred to the reference inflow wind speed u_{ref}=11.5m/s upstream of T1 and the red, orange and yellow point the optimum power point when the turbines are individually controlled for optimum power output.

Fig.2 (b) shows the relative power of the second and third row turbine relative to the optimum power output of the front row turbine. The measured powers show good agreement to a dataset of full scale measurements and LES simulations at Lillgrund wind farm, which was presented by Nilsson et al [9]. The Lillgrund wind farm is a tightly spaced wind farm with an inter-turbine spacing of 4.3D in SW-NE direction respectively 3.3D in SE-NW direction, making it a convenient reference case for the presented model scale setup. For this comparison, only the outermost row furthest to NE with a separation distance of 3.3D is considered (row A, Nilsson et al. [9]). Only one side of this row is interacting with the wake flow from adjacent rows while the other side is exposed to the undisturbed freestream flow.

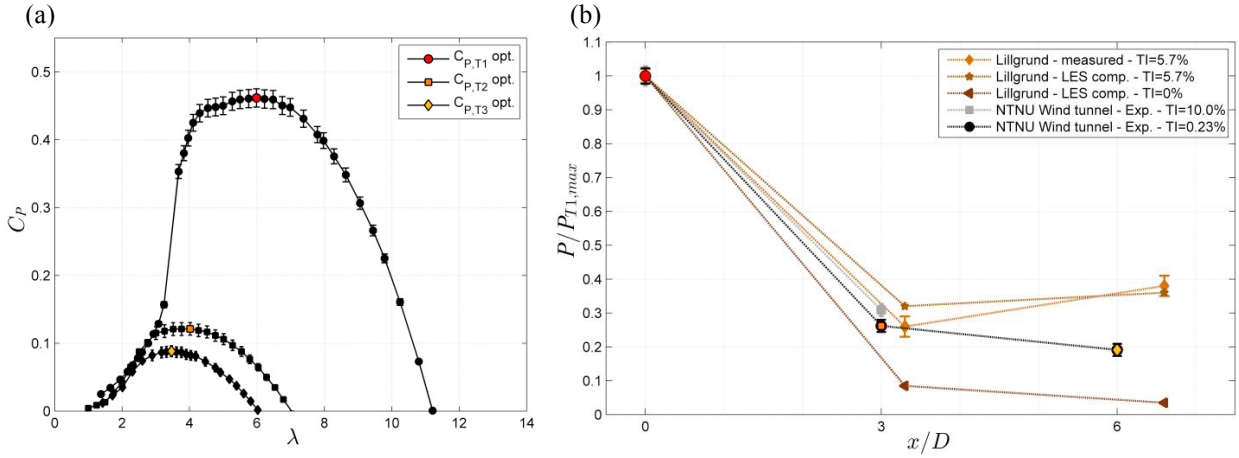

Fig. 2. (a) C_P-λ-curves of the three aligned turbines, their optimum points (red, orange, yellow); all referred to u_{ref}=11.5m/s (b) relative power of test cases compared to full-scale data from Lillgrund windfarm [Nilsson et al., 9]

The relative power of second turbine in this experiment with 0.23% inflow turbulence matches the measured value from Lillgrund with a background turbulence of 5.7% very well. Large Eddy Simulations (LES) by Nilsson et al. [9] with no background turbulence (TI=0%) resulted in significantly lower power outputs for the second turbine, which are considered to be unrealistically low.

In order to reproduce more realistic atmospheric conditions, the power of the second turbine was also measured for a grid generated turbulence of TI=10.0%. This resulted in an 18% higher power output for the second turbine compared to the low turbulent inflow of TI=0.23%. This is consistent with findings of Churchfield et al. [14], who performed LES simulations on two aligned full-scale 5MW turbines in atmospheric boundary layers of different stability. They found 15-20% higher power production of the second row turbine for highly turbulent unstable conditions than for neutral conditions featuring lower background turbulence.

The measured power output of the third row turbine, however, is significantly lower than the measured power from Lillgrund wind farm. In fact the power drops about 27% from the second to the third turbine, while it increases with about 46% in the measured full scale data. This noteworthy power increase is considered to stem from a strong re-energizing of the turbulent wake. As the background turbulence for the wind tunnel case is considerably lower, the wake does not re-energize as fast and the power of the third row is lower. A similar power drop from the second to the third turbine is observed in the LES computations by Nilsson et al [9] for zero inlet turbulence.

3.2. Effects of power curtailment

According to momentum theory, a reduction of the front turbine's induction benefits the total power production of a number of aligned turbines. The curtailment of a turbine can be done by blade pitching or a variation away from its optimum tip speed ratio. In [5], Bartl and Sætran showed that curtailment through tip speed variation is the more promising option with respect to total power gains. For an operation at lower than rated tip speed ratios more kinetic energy is left in the center of the wake compared to the pitching case [5].

3.2.1. Front row turbine curtailment

At first, the effects of a curtailment of the first turbine are analyzed. Fig. 3 (a) shows the C_P-λ characteristics of the second row turbine for four cases of first row turbine curtailment. In three cases T1 is slowed down, in one case slightly overspeeded. It is observed that the second turbine is able to recover about the same amount of energy that is lost through curtailment of the first turbine. The exact numerical values of the relative power measured are tabulated in Table 1.

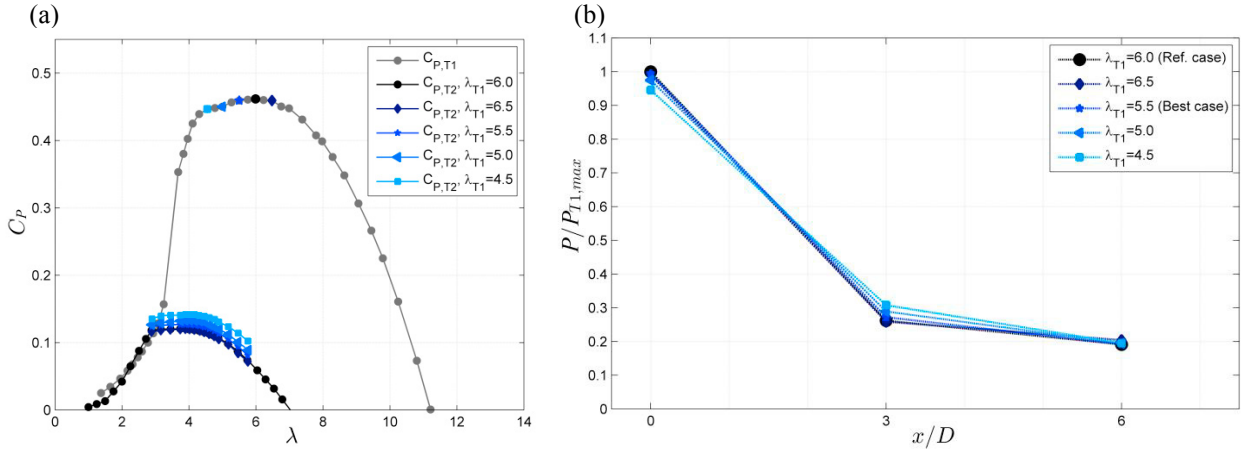

Fig. 3. (a) C_P-λ-curves of the second turbine T2 depending on different tip speed ratios of T1
(b) relative power for T1, T2 and T3 for a curtailed first row turbine T1

In Fig 3 (b) the relative power for all three turbine rows for cases when the front row turbine T1 is operated at off-design condition is presented. Turbines T2 and T3 are for these cases always controlled to their individual maximum power point. As indicated in the last two columns in Table 1, the combined power output of the three aligned turbines is observed to be very constant for these four cases of front row curtailment. Only very small gains in total power of less than one percent can be achieved. Although these power gains are insignificant considering a statistical measurement uncertainty of the same magnitude, the best gains are measured for tip speed ratios slightly lower than the rated TSR at λ_{T1}=6.0. Overspeeding to λ_{T1}=6.5 is observed to have a somewhat negative effect on the total power production.

Remarkably, the power produced by the third row turbine T3 is observed to be very constant for all cases of front row turbine curtailment. In these test cases it seems that most of the kinetic energy lost at the front row turbine due to curtailment is recovered by the second row turbine. The third turbine's production is rather unaffected, although the upstream turbine is extracting somewhat more energy from the flow.

Table 1. Total array power and operating points for five cases of first row turbine curtailment

λ_{T1}	$P_{T1}/P_{T1,max}$	λ_{T2}	$P_{T2}/P_{T1,max}$	λ_{T3}	$P_{T3}/P_{T1,max}$	$P_{T1+T2+T3}/P_{T1,max}$	+/- in %
6.0	1.0000	4.0	0.2620	3.5	0.1913	1.4533	-
5.5	0.9948	3.7	0.2721	3.5	0.1919	1.4588	+0.38%
5.0	0.9749	4.0	0.2892	3.5	0.1945	1.4587	+0.37%
4.5	0.9456	3.9	0.3075	3.3	0.2026	1.4558	+0.17%
6.5	0.9903	3.9	0.2607	3.3	0.2018	1.4527	-0.04%

3.2.2. Second row turbine curtailment

In another set of test cases the second row turbine T2 is curtailed while the first turbine T1 is constantly operated at its rated tip speed λ_{T1}=6.0. In Fig. 4 (a) the C_P-λ characteristics of the third row turbine T3 are presented for four operating points λ_{T2}=[2.0, 3.7, 4.0, 6.0] of the second turbine. λ_{T2}=4.0 represents the reference case at which the second turbine is controlled to its maximum power point. Curtailing the second turbine to a slightly lower than optimum tip speed ratio of λ_{T2}=3.7 results in the best combined power production of these cases. A gain in total power production $P_{T1+T2+T3}$ of 0.09% as shown in Table 2, however, is even less significant than the gains achieved for the first turbine curtailment. The other two cases of λ_{T2}=2.0 and λ_{T2}=6.0 represent two cases of more distinct curtailment of the second row turbine T2.

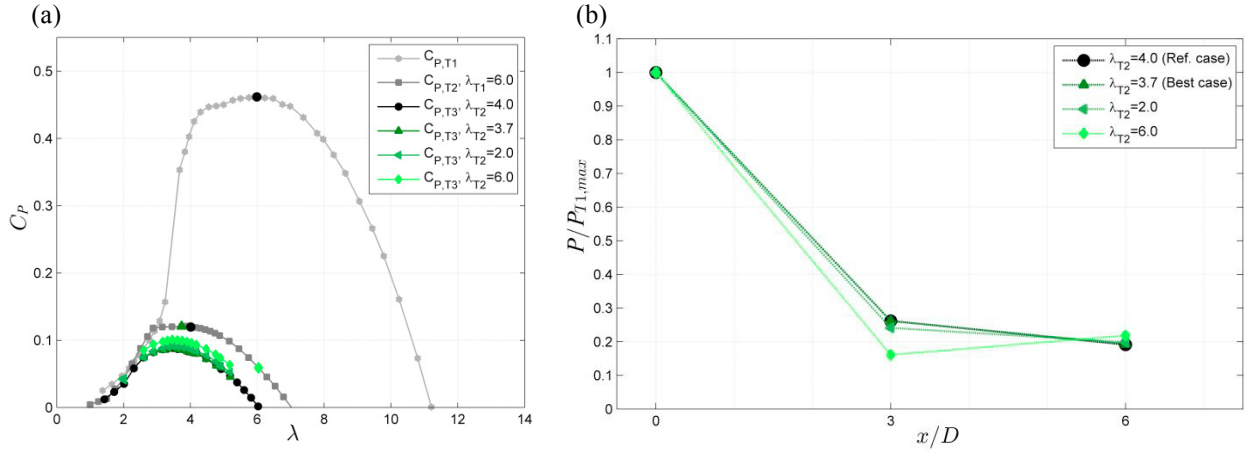

Fig. 4. (a) C_P-λ-curves of the third turbine T3 depending on different tip speed ratios of T2
(b) relative power for T1, T2 and T3 for a curtailed second row turbine T2

For λ_{T2}=2.0 the relative power of T2 is curtailed by about 2% of the relative power $P_{T2}/P_{T1,max}$, of which about 0.7% can be recovered by the third turbine T3. The losses in total array power are calculated to amount -0.92%, which is surprisingly little for this slowdown of half the rotational speed. For overspeeding the second turbine to λ_{T2}=6.0 about 10% less relative power $P_{T2}/P_{T1,max}$ is produced by T2. Accordingly, about 2.7% of relative power can be recovered by T3. The total power loss for this overspeeding case of -5.09% is significantly bigger than for the slowdown case. In order to understand the mechanisms behind the power production of the single turbine rows, the wake flow between the turbines has to be analyzed.

Table 2. Total array power and operating points for five cases of second row turbine curtailment

λ_{T1}	$P_{T1}/P_{T1,max}$	λ_{T2}	$P_{T2}/P_{T1,max}$	λ_{T3}	$P_{T3}/P_{T1,max}$	$P_{T1+T2+T3}/P_{T1,max}$	+/- in %
6.0	1.0000	4.0	0.2620	3.5	0.1913	1.4533	-
6.0	1.0000	3.7	0.2616	3.5	0.1931	1.4547	+0.09%
6.0	1.0000	2.0	0.2414	3.5	0.1986	1.4399	-0.92%
6.0	1.0000	6.0	0.1609	3.5	0.2185	1.3793	-5.09%

3.3. Wake flow analysis

A set of Laser-Doppler Anemometry (LDA) measurements at x/D=3 rotor diameters behind the first row as well as behind the second row turbine is performed in order to assess which inflow conditions each of the turbines in the array experiences. The wake flow is recorded in the exact same locations of the second respectively the third turbine without the second/third turbine being installed in the wind tunnel. The flow field is therefore considered representative for the inflow conditions, which the second/third turbine row experiences.

In Fig. 5 (a) and (b) the normalized mean velocity fields in the wake x/D=3 behind the first row turbine T1 and the second row turbine T2 are compared with the reference case (λ_{T1}=6.0, λ_{T2}=4.0). The wake behind the second row features a somewhat higher velocity deficit in the center of the wake than the wake behind the first row turbine, which is considered the main reason for a further drop in power from the second to the third turbine row. The wake behind T2 is more shaped like a bell compared to the steep velocity gradients around z/R=±1 and rather flat central area in the wake center for the wake behind T1.

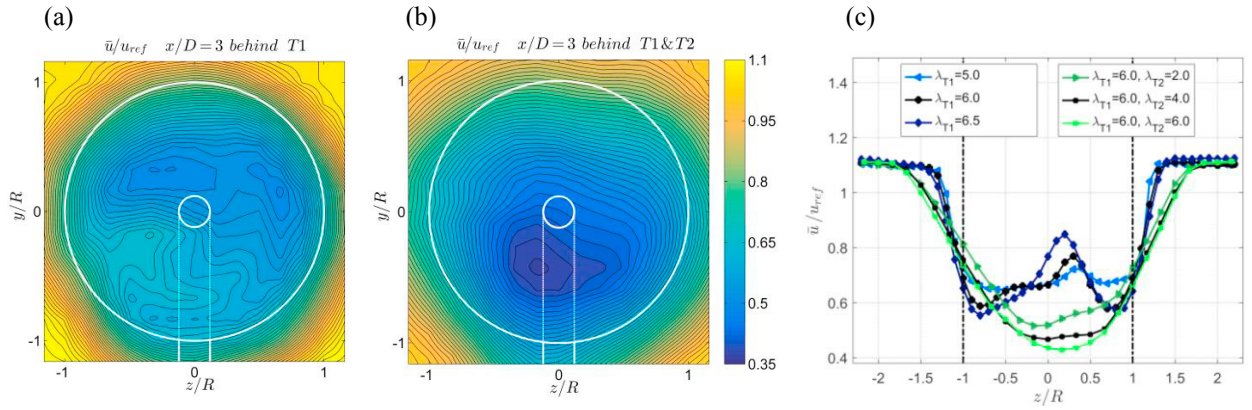

Fig. 5. Normalized mean velocity in the wake x/D=3
(a) behind T1 operated at λ_{T1}=6 (reference case);
(b) behind T2 while T1 operated at λ_{T1}=6 and T2 operated at λ_{T2}=4 (reference case);
(c) behind T1 operated at λ_{T1}=5,6,7 (blue lines are the curtailed cases) respectively
behind T2 while T1 operated at λ_{T1}=6 and T2 operated at λ_{T2}=2,4,6 (green lines are the curtailed cases)

Fig. 6 (a) and (b) show the corresponding plots of normalized turbulent kinetic energy in the wake. The peaks in TKE behind the second turbine are slightly higher in the lower half of the wake, but generally feature the same magnitude as the wake behind the first turbine. The main difference is the more spread out TKE in the wake of T2, while the first turbine wake features very sharp distinct TKE peaks around in the blade tip region. The rotor generated turbulence of T1 is somewhat diffused at the T2 position and superimposed by the rotor generated turbulence of T2. Due to the more spread out turbulence distribution in the second turbine wake, the mixing and entrainment of higher kinetic energy freestream flow are increased resulting in a faster wake recovery [6].

In Fig. 5 (c) normalized mean velocity profiles measured at hub height behind the curtailed first (blue lines) and second row turbine (green lines) are compared to the velocity profiles of the reference case (black lines). When the first turbine is overspeeded to λ_{T1}=6.5 more energy is taken out of the flow in the regions close to the blade tip, while more energy is left in the flow in the center of the wake. The opposite effect is observed in the wake of the turbine curtailed to λ_{T1}=5.0. Less energy is extracted in the blade tip regions, and a much flatter wake profile is formed behind the rotor. The corresponding profiles of normalized turbulent kinetic energy are shown in Fig. 6 (c). Herein, the TKE peaks in the shear layer are observed to be slightly reduced for smaller first turbine tip speed ratios.

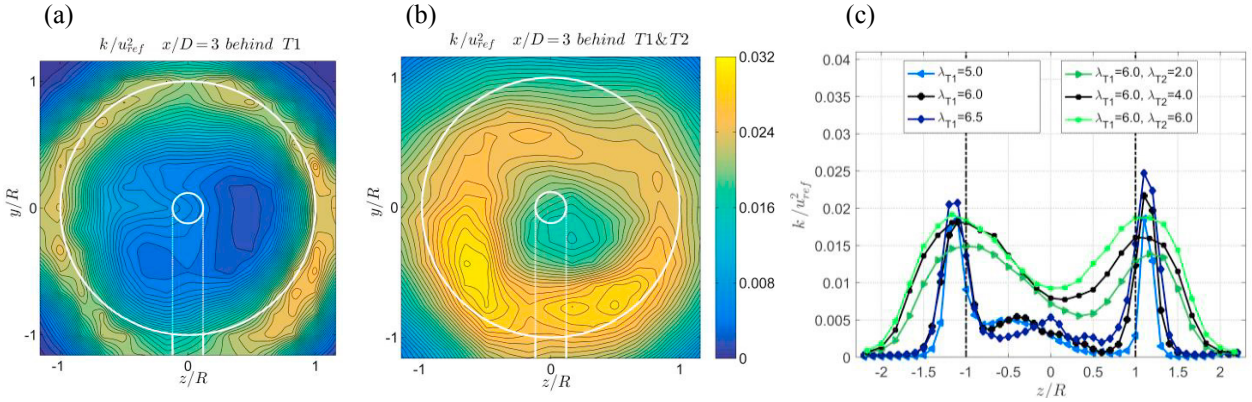

Fig. 6. Normalized turbulent kinetic energy in the wake x/D=3
(a) behind T1 operated at λ_{T1}=6 (reference case);
(b) behind T1 operated at λ_{T1}=6 and T2 operated at λ_{T2}=4 (reference case);
(c) behind T1 operated at λ_{T1}=5,6,7 (blue lines are the curtailed cases) respectively
behind T1 operated at λ_{T1}=6 and T2 operated at λ_{T2}=2,4,6 (green lines are the curtailed cases)

The two cases of more distinct curtailment of the second turbine are shown in the green profiles in Fig 5 (c) and 6 (c). Curtailment to a lower T2 tip speed ratio λ_{T2}=2.0 is observed to somewhat increase the kinetic energy left in the wake. This is not reflected in power measurements on the third row turbine, which is able to extract about the same amount of energy as for the reference case. An increase of the second turbine tip speed ratio to λ_{T2}=6.0 is observed to slightly reduce the mean velocity in the wake even further. This observation is in contradiction to a slightly higher power output for T3. The turbulence levels in the wake behind the second turbine are observed to be higher for higher tip speed ratios.

4. Conclusions

A comparison of the power outputs of the three first rows shows good agreement with measurements from a full-scale wind farm of similar inter-turbine spacing. As observed in most full-scale wind farms, the power drop from the first to the second row is a considerably bigger than the power drop from the second to the third row. A comparison of the wake flow behind the first row and second row shows a significantly higher mean velocity loss behind the second row justifying the further power drop from the second to the third row turbine. Furthermore, the time-averaged turbulent kinetic energy production behind the second turbine is spread out further into freestream and center of the wake than for the first turbine wake. The higher turbulence levels contribute to increased mixing and faster wake recovery behind the second turbine.

Curtailing the front row turbine to smaller tip speed ratios only resulted in very small total power gains below 1%, which is insignificant considering a statistical measurement uncertainty of the same magnitude. Curtailments of both the first and second row turbine indicate that the best combined array power results are achieved for slightly lower than rated tip speed ratios. Although tip speed ratio curtailment seems to have a rather small potential for a wind farm power optimization, it could be an effective method to distribute loads between the turbine rows as an operation at a rather constant array power seems possible over a wide range of tip speed ratios.

References

[1] Barthelmie RJ, Frandsen ST, Hansen K, Schepers JG, Rados K, Schlez W, Neubert A, Jensen LE, Neckelmann S. Quantifying the Impact of Wind Turbine Wakes on Power Output at Offshore Wind Farms. *J Atmos Oceanic Technol 2010*;27:1302-1317.
[2] Knudsen T, Bak T, Svenstrup M. Survey of wind farm control - power and fatigue optimization. *Wind Energy 2014*;18:1333-1351.
[3] Adaramola MS, Krogstad PÅ. Experimental investigation of wake effects on wind turbine performance. *Renew Energy 2011*;36:2078-2086.
[4] Campagnolo F, Petrović V, Schreiber J, Nanos EM, Croce A, Bottasso CL. Wind tunnel testing of a closed-loop wake deflection controller for wind farm power maximization. *JPCS 2016*;753.
[5] Bartl J, Sætran L. Experimental testing of axial induction based control strategies for wake control and wind farm optimization. *JPCS 2016*;753:032035
[6] Hansen KS, Barthelmie RJ, Jensen LE, Sommer A. The impact of turbulence intensity and atmospheric stability on power deficits due to wind turbine wakes at Horns Rev wind farm. *Wind Energy 2012*;15:183–196.
[7] Ceccotti C, Spiga A, Bartl J, Sætran L. Effect of upstream turbine tip speed variations on downstream turbine performance. *Energy Procedia 2016*;94C:478-486.
[8] Frandsen S, Barthelmie R, Pryor S, Rathmann O, Larsen S, Højstrup J, Thøgersen M. Analytical modelling of wind speed deficit in large offshore wind farms, *Wind Energy 2006*;9:39-53.
[9] Nilsson K, Ivanell S, Hansen KS, Mikkelsen R, Sørensen JN, Breton S-P, Henningson D. Large-eddy simulations of the Lillgrund wind farm. *Wind Energy 2015*;18:449–467
[10] Mikkelsen R, Sørensen JN, Øye S, Troldborg N. Analysis of power enhancement for a row of wind turbines using the actuator line technique. *JPCS 2007*;75:012044.
[11] Ostovan Y, Amiri H, Uzol O. Aerodynamic Characterization of NREL S826 Airfoil at Low Reynolds Numbers, *RUZGEM 2013*.
[12] Sarmast S, Mikkelsen R. The experimental results of the NREL S826 airfoil at low Reynolds numbers. *Technical Report, urn:nbn:se:kth:diva-120583, 2013*.
[13] Sagmo KF, Bartl J, Sætran L. Numerical simulations of the NREL S826 airfoil. *JPCS 2016*;753:082036.
[14] Churchfield MJ, Lee S, Michalakes J, Moriarty PJ. A numerical study of the effects of atmospheric and wake turbulence on wind turbine dynamics. *Journal of Turbulence 2012*;13:N14.